Cullin neddylation inhibitor attenuates hyperglycemia by enhancing hepatic insulin signaling through insulin receptor substrate stabilization

Cheng Chen[a,1], Lijie Gu[a,1], David J. Matye[a,b], Yung-Dai Clayton[a], Mohammad Nazmul Hasan[a], Yifeng Wang[b], Jacob E. Friedman[a], and Tiangang Li[a,b,2]

[a]Harold Hamm Diabetes Center, Department of Physiology, University of Oklahoma Health Sciences Center, Oklahoma City, OK 73104; and [b]Department of Pharmacology, Toxicology, and Therapeutics, University of Kansas Medical Center, Kansas City, KS 66160

Edited by C. Ronald Kahn, Research, Harvard Medical School, Boston, MA; received June 24, 2021; accepted December 27, 2021

Hepatic insulin resistance is a hallmark feature of nonalcoholic fatty liver disease and type-2 diabetes and significantly contributes to systemic insulin resistance. Abnormal activation of nutrient and stress-sensing kinases leads to serine/threonine phosphorylation of insulin receptor substrate (IRS) and subsequent IRS proteasome degradation, which is a key underlying cause of hepatic insulin resistance. Recently, members of the cullin-RING E3 ligases (CRLs) have emerged as mediators of IRS protein turnover, but the pathophysiological roles and therapeutic implications of this cellular signaling regulation is largely unknown. CRLs are activated upon cullin neddylation, a process of covalent conjugation of a ubiquitin-like protein called Nedd8 to a cullin scaffold. Here, we report that pharmacological inhibition of cullin neddylation by MLN4924 (Pevonedistat) rapidly decreases hepatic glucose production and attenuates hyperglycemia in mice. Mechanistically, neddylation inhibition delays CRL-mediated IRS protein turnover to prolong insulin action in hepatocytes. In vitro knockdown of either cullin 1 or cullin 3, but not other cullin members, attenuates insulin-induced IRS protein degradation and enhances cellular insulin signaling activation. In contrast, in vivo knockdown of liver cullin 3, but not cullin 1, stabilizes hepatic IRS and decreases blood glucose, which recapitulates the effect of MLN4924 treatment. In summary, these findings suggest that pharmacological inhibition of cullin neddylation represents a therapeutic approach for improving hepatic insulin signaling and lowering blood glucose.

insulin resistance | cullin | MLN4924 | diabetes | fatty liver

A Cullin-RING E3 ligase (CRL) is a multiprotein complex generally consisting of a cullin protein, a RING E3 ligase, and a substrate receptor that recognizes specific substrates for ubiquitination and proteasomal degradation (1). Each of the cullin member proteins serves as the scaffold of a functionally distinct CRL complex. Mammalian cells express a large number of substrate receptors in a tissue-specific manner, which further determines the substrate specificity of a unique CRL complex. CRLs are activated upon cullin neddylation, a process of covalent conjugation of a ubiquitin-like protein called Nedd8 to a conserved lysine on a cullin protein (1). Neddylation is mediated by a set of specialized Nedd8 E1, E2, and E3 enzymes that sequentially transfer Nedd8 to a cullin protein. Unlike protein ubiquitination, current knowledge supports that cullin proteins are the predominant neddylation targets in mammalian cells (2). Recently, CRLs have emerged as attractive targets for drug development (3). In the last 10 y, CRLs have drawn major attention in cancer research owing to CRL regulation of oncogenes and tumor suppressors (4). The Nedd8-activating E1 enzyme (NAE1) is the only known Nedd8 E1 enzyme (1). MLN4924 (Pevonedistat) is the first in-class small molecule inhibitor of NAE1 and has entered Phase-I/II clinical trials for various cancer treatments (5). In contrast, the translational potential of targeting cullin neddylation for treating other diseases is still largely unknown.

Hepatic insulin resistance is a hallmark pathogenic feature of fatty liver disease and type-2 diabetes, and decreased hepatocellular insulin receptor substrate (IRS) is a key underlying cause (6, 7). Following insulin activation, IRS signaling is feedback inactivated by mechanistic target of rapamycin (mTOR)-mediated serine/threonine phosphorylation and subsequent IRS proteosome degradation (8, 9). Although this feedback mechanism prevents sustained insulin signaling activation in cells, overactivation of this desensitization mechanism by mTOR and other stress/nutrient kinases significantly contributes to hepatic insulin resistance in fatty livers (8, 10). However, the broad cellular functions of these kinases present a major obstacle in targeting them to prevent insulin resistance (11). Serine/threonine-phosphorylated IRS proteins are destined for ubiquitylation and proteasome degradation (9, 12), but targeting the proteasome pathway is unlikely a viable approach due to the perceived broad biological impact. Interestingly, studies of mouse embryonic fibroblasts have revealed that CRLs are involved in mediating IRS1 protein turnover (13, 14). These findings prompted us to ask two intriguing questions: First, are CRLs involved in regulating hepatic insulin signaling, and if yes, which CRL may mediate such an effect in hepatocytes? Second, can CRLs serve as potentially new therapeutic targets for modulating insulin signaling and glucose homeostasis in fatty liver disease in vivo? Here, we report findings that neddylation inhibition effectively

Significance

Hepatic insulin resistance is a well-recognized cause of hepatic glucose overproduction and fasting hyperglycemia in fatty liver disease and type-2 diabetes. Here, we have discovered that pharmacological inhibition of cullin neddylation by NAE1 inhibitor enhances hepatic insulin signaling and lowers blood glucose in mice. Hepatic neddylation inhibition delays cullin-RING E3 ligase–mediated insulin receptor substrate protein degradation and thus directly targets a key pathogenic defect underlying hepatic insulin resistance. This finding suggests that targeting cullin neddylation may be a potential therapeutic strategy for treating hyperglycemia.

Author contributions: C.C., L.G., and T.L. designed research; C.C., L.G., D.J.M., Y.-D.C., M.N.H., Y.W., and T.L. performed research; C.C., L.G., and T.L. analyzed data; J.E.F. and T.L. wrote the paper; and J.E.F. performed critical revision of the manuscript.

The authors declare no competing interest.

This article is a PNAS Direct Submission.

[1]C.C. and L.G. contributed equally to this study.

[2]To whom correspondence may be addressed. Email: tiangang-li@ouhsc.edu.

This article contains supporting information online at http://www.pnas.org/lookup/suppl/doi:10.1073/pnas.2111737119/-/DCSupplemental.

Published February 3, 2022.

enhances hepatic insulin signaling by delaying CRL-mediated IRS turnover, resulting in attenuated hyperglycemia in obese mice.

Results

Neddylation Inhibition Prolongs Insulin Action by Stabilizing IRS Protein in Hepatocytes. To determine the effect of neddylation inhibition on hepatic insulin signaling, we first measured the key components of the insulin signaling cascade in MLN4924-treated mouse liver AML12 cells and primary hepatocytes. Under insulin-stimulated conditions, MLN4924 dose dependently increased total IRS1 and IRS2 protein but not total insulin receptor (IR) or AKT (Fig. 1*A*). This resulted in increased AKT(S473) phosphorylation that correlated with enhanced IRS1(Y612) phosphorylation but not IR (Y1150) phosphorylation (Fig. 1*A*). This MLN4924-mediated effect is highly dose dependent, and a partial neddylation inhibition was sufficient to enhance hepatic insulin signaling activation (Fig. 1*A*). Similar effects were observed in primary human hepatocytes (Fig. 1*B* and *SI Appendix*, Fig. S1*A*) and primary mouse hepatocytes (*SI Appendix*, Fig. S1*B*), which ruled out a cell-type–specific effect. When cells were stimulated with insulin in time course, the presence of MLN4924 significantly delayed insulin signaling desensitization at the IRS1(Y612) and AKT(S473) levels in AML12 cells and primary mouse hepatocytes (Fig. 1*C* and *SI Appendix*, Fig. S1*B*). This effect was not associated with IR (Y1150) phosphorylation but was explained by higher IRS protein abundance. Activation of mTORC1 downstream of insulin signaling mediates IRS1 serine phosphorylation and subsequent ubiquitin–proteasomal degradation (8). In the presence of MLN4924, IRS1 S307 phosphorylation was also higher (Fig. 1*C*), suggesting that delayed IRS1 inactivation was due to delayed IRS1 protein degradation but not reduced IRS1 serine phosphorylation. Similarly, treatment of a different neddylation inhibitor, TAS4464, decreased cullin neddylation, stabilized IRS protein, and enhanced AKT activation (Fig. 1*D*) (15). When cycloheximide (CHX) was used to block protein synthesis, insulin-induced IRS degradation appeared to be rapid in vehicle-treated cells and was significantly delayed by MLN4924 (Fig. 1 *E* and *F*). In contrast, other proteins including AKT, Cul3, and NAE1 appeared to be more stable (Fig. 1*E*). Under insulin-stimulated condition, blocking the mTORC1-mediated IRS feedback inhibition by rapamycin decreased IRS1 serine phosphorylation (lower IRS1(S307) phosphorylation and lack of insulin-induced IRS band shift) and increased IRS protein to similar levels in MLN4924-treated cells (Fig. 1*G*). MLN4924 did not further increase IRS protein in the presence of rapamycin (Fig. 1*G*), supporting that mTORC1-mediated serine/threonine phosphorylation of IRS and CRL-mediated degradation are two sequential steps in the same insulin-desensitization mechanism. These rapamycin effects on IRS proteins could be reproduced by using a PI3K inhibitor wortmannin and a TORC1/2 inhibitor Torin 1, both of which blocked downstream mTOR activation, except that both inhibitors also decreased downstream AKT activation owing to the known roles of PI3K and TORC2 in mediating AKT phosphorylation (*SI Appendix*, Fig. S2 *A* and *B*). In summary, these findings suggest that CRL inhibition enhances hepatocellular insulin signaling by delaying IRS protein turnover. CRL inhibition did not cause persistent AKT activation in the absence of insulin but rather slowed insulin signaling feedback desensitization, which may be especially relevant under hepatic insulin-resistant conditions to enhance hepatic responsiveness to higher circulating insulin.

CRL Inhibition Enhances Hepatic Insulin Signaling and Reduces Hepatic Glucose Production. We next administered MLN4924 to chow-fed mice via subcutaneous (SQ) injection (5 PM on day 1 and 9 AM on day 2) to further determine the in vivo effect of neddylation inhibition. The dose of 60 mg/kg is generally in line with published literature (16). MLN4924 treatment effectively reduced hepatic cullin neddylation (Fig. 2 *A* and *B*). Consistent with our in vitro findings, MLN4924 increased hepatic IRS proteins and AKT phosphorylation (Fig. 2 *A* and *B*). A pyruvate tolerance test (PTT) and glucose tolerance test (GTT) revealed significantly reduced hepatic glucose production and improved overall glucose tolerance in mice fed chow diet or a brief 4-wk Western diet (WD) feeding (Fig. 2 *C*–*F*). Notably, the peak blood glucose at 30 min was significantly lower in mice treated with MLN4924, which consistently supports hepatic action of MLN4924 in reducing glucose production. In addition to liver, skeletal muscle is another organ that quantitatively contributes to plasma glucose homeostasis. However, MLN4924 did not inhibit skeletal muscle cullin neddylation or alter IRS protein abundance or AKT phosphorylation, possibly due to very limited drug distribution to skeletal muscle (*SI Appendix*, Fig. S3 *A* and *B*). Furthermore, the insulin tolerance test (ITT) showed that, despite lower basal glucose in the MLN4924-treated WD-fed group, both groups showed similarly decreased plasma glucose to ∼25 mg/dL in response to insulin after 1 h (*SI Appendix*, Fig. S3*C*), indicating the two groups have similar muscle glucose uptake in response to insulin stimulation.

Cullin 1 and 3 Mediate IRS Protein Degradation in Hepatocytes. To identify the cullin members that are involved in IRS regulation, we performed a screening experiment by specifically knocking down each of the six mammalian canonical cullins (Cul1, Cul2, Cul3, Cul4A, Cul4B, and Cul5) and the atypical Cul7 in AML12 cells (Fig. 3*A*). Knockdown of each cullin at the protein level (except Cul5 due to the lack of a working antibody from commercial sources) was confirmed by Western blotting (*SI Appendix*, Fig. S4*A*). Under insulin-stimulated conditions that induced rapid IRS protein degradation within 6 h (Fig. 1*C*), knockdown of Cul1 or Cul3 appeared to delay IRS turnover (Fig. 3*B* and *SI Appendix*, Fig. S4*B*). Knockdown of other cullins, including Cul7, which was previously reported to regulate IRS1 in mouse embryonic fibroblasts (13), did not affect IRS stability (*SI Appendix*, Fig. S4*B*), indicating that a CRL complex exhibits cell-type–specific functions. Knockdown of either Cul1 or Cul3 increased cellular response to insulin-stimulated AKT activation and thus recapitulated the effect of MLN4924 (Fig. 3 *C* and *D*). These results also showed that the loss of either Cul1 or Cul3 was not fully compensated for by the other cullin, implying that at least in liver cells, Cul1 and Cul3 may function in an additive manner to mediate rapid IRS turnover. In Cul1 or Cul3 knockdown cells, further MLN4924-mediated IRS enrichment and insulin sensitization appeared to be limited but not fully abolished (*SI Appendix*, Fig. S5 *A*–*C*), likely due to neddylation inhibition on the remaining Cul1 and Cul3. Simultaneous knockdown of Cul1 and Cul3 largely abolished further IRS protein stabilization caused by MLN4924 (Fig. 3*E*). In further support, simultaneous Cul1 and Cul3 knockdown significantly delayed insulin-stimulated IRS protein degradation when protein synthesis was blocked by CHX (Fig. 3 *F* and *G*).

To seek further supporting evidence that Cul1 and Cul3 mediate IRS turnover, we next performed coimmunoprecipitation (Co-IP) assays to determine if IRS coprecipitates with Cul1 and/or Cul3. Because only a very small percentage of total cellular Cul1 or Cul3 is expected to interact with IRS and such interaction may be transient due to subsequent IRS dissociation and proteosome degradation, we expressed FLAG-tagged Cul1 or Cul3 using adenovirus in AML12 cells to increase the bait protein IP yield (Fig. 4 *A* and *B*) and also pretreated cells with the proteasome inhibitor MG132 to prevent IRS degradation. The Co-IP experiment showed that IRS1 was coimmunoprecipitated with Cul1 and Cul3 (Fig. 4 *C* and *D*). To further determine if these

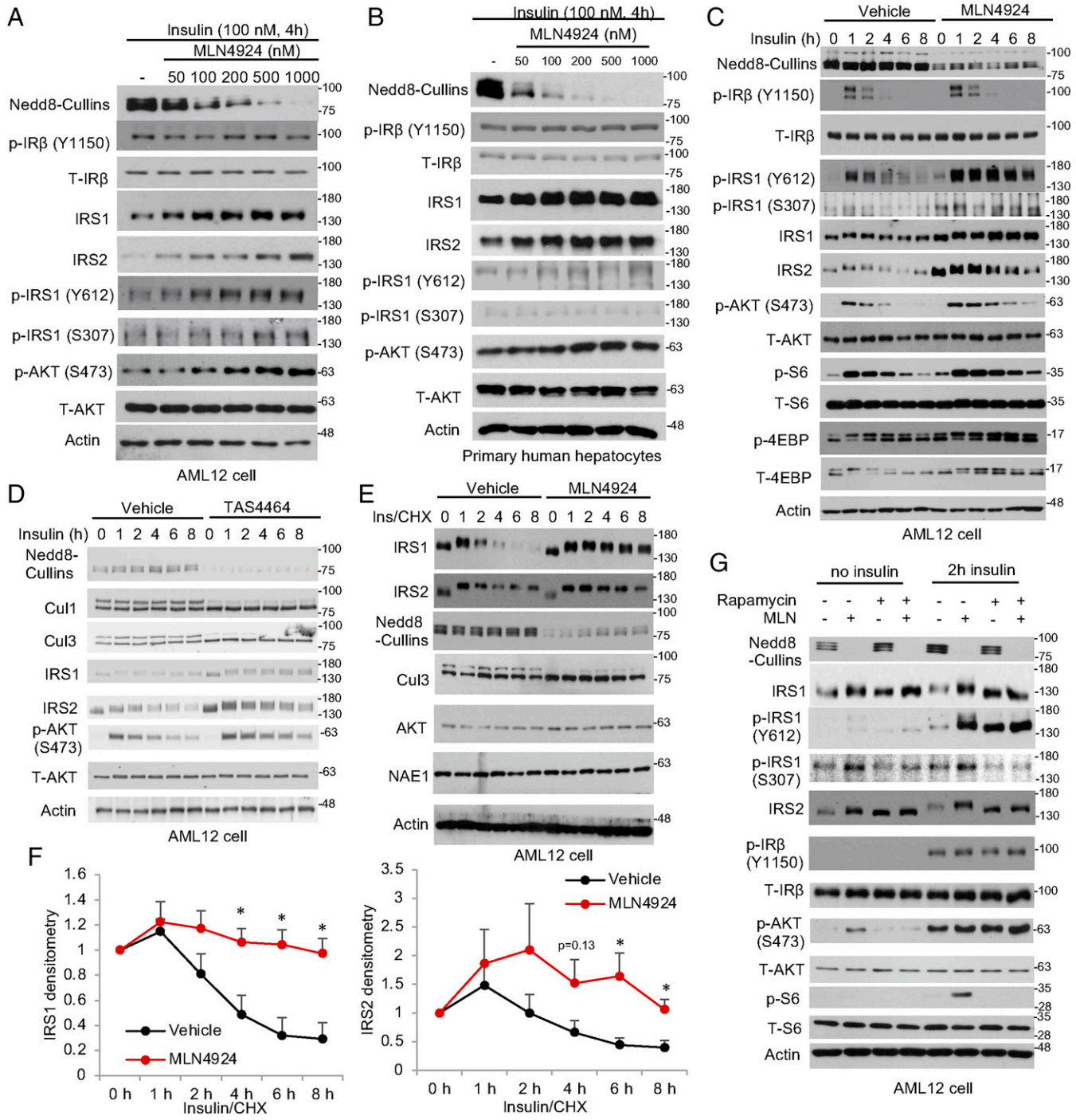

Fig. 1. MLN4924 enhances hepatocyte insulin sensitivity by delaying feedback IRS degradation. (*A* and *B*) Western blot. Cells were serum starved for 16 h. Cells were then pretreated with MLN4924 for 1 h followed by insulin stimulation for 4 h. (*C* and *D*) Western blot. AML12 cells were serum starved for 16 h. Cells were then pretreated with 500 nM MLN4924 or 200 nM TAS4464 for 1 h followed by 100 nM insulin stimulation in time course. (*E*) Western blot. AML12 cells were serum starved for 16 h. Cells were then pretreated with 500 nM MLN4924 or vehicle (dimethylsulfoxide [DMSO]) for 1 h, followed by 100 μg/mL CHX and 100 nM insulin (ins) treatment. (*F*) Densitometry of IRS protein as in *E*. Mean ± SEM of three independent experiments. $*P < 0.05$ versus Vehicle at the same time point. Unpaired Student's *t* test. (*G*) Western blot. AML12 cells were serum starved for 16 h. Cells were pretreated with 100 nM rapamycin and 500 nM MLN4924 as indicated for 1 h followed by additional 2-h incubation in the presence or absence of 100 nM insulin.

interactions are affected by insulin, some cells were stimulated with insulin for 2 h before cell lysis. However, co-IP results did not indicate that these interactions were clearly enhanced by insulin possibly due to the dynamic and transient nature of the CRL–substrate interaction (Fig. 4 *E* and *F*) (17).

It has been shown that only a fraction of each cullin is in active CRL complexes in cells, and in addition to the dynamic neddylation–deneddylation cycles, the relative abundance of substrate receptors also plays an important role in regulating CRL–substrate engagement (17). FBXW8 is an F-box protein

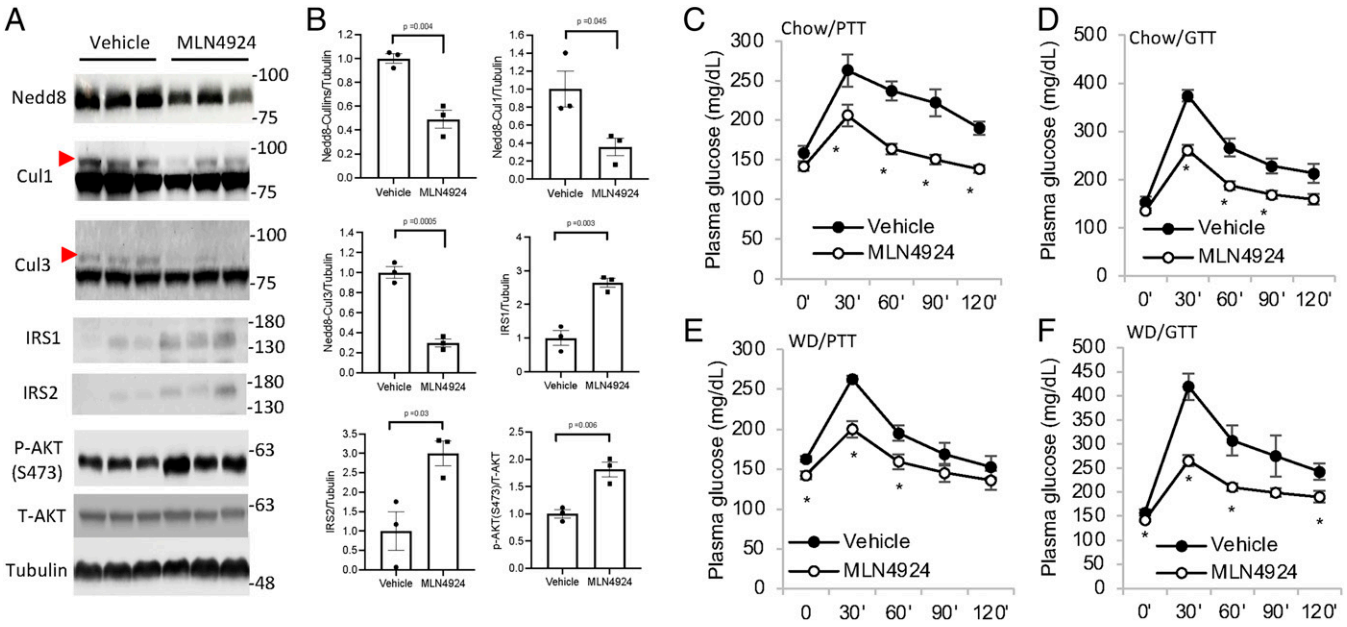

Fig. 2. MLN4924 treatment acutely decreases hepatic glucose production in mice. (*A* and *B*) Male C57BL/6J mice were treated with 60 mg/kg MLN4924 via SQ injection at 5 PM on day 1 and 9 AM on day 2. Mice were fasted from 9 AM to 3 PM on day 2 and euthanized. Effect of MLN4924 on hepatic cullin neddylation was measured by Western blotting shown in *A*. Densitometry is shown in *B*. The red arrows indicate neddylated cullin bands. (*C–F*) Male C57BL/6J mice on chow diet (*C* and *D*) or WD for 4 wk (*E* and *F*) were administered 60 mg/kg MLN4924 as described in *A*. PTT or GTT were performed as described in *Materials and Methods*. Results are expressed as mean ± SEM (n = 4 to 5). *$P < 0.05$ versus Vehicle group at the same time point. Unpaired Student's t test was used to calculate the P value.

substrate receptor that has previously been shown to mediate Cul7 interaction with IRS1 in mouse embryonic fibroblast cells (13). Although knockdown of Cul7 does not affect IRS1 turnover in liver cells, it is known that CRL1 recruits F-box proteins as its substrate receptors (1, 4). Indeed, we found that FBXW8 was also coprecipitated with Cul1 but not Cul3 (Fig. 4*G*). Furthermore, knockdown of FBXW8 stabilized IRS protein and enhanced insulin activation of AKT (Fig. 4*H*). These results suggest that FBXW8 also acts as a CRL1 substrate receptor to mediate IRS degradation. In contrast, CRL3 mainly recruits BTB-domain proteins as substrate receptors (1, 4). Although over 100 BTB proteins can potentially serve as Cul3 substrate receptors to mediate CRL3 recognition of various cellular substrates, a recent study using BioID screening has identified Kelch-like proteins KLHL9 and KLHL13, two previously reported CRL3 substrate receptors (18), as IRS1-recognizing CRL3 substrate receptors in mouse embryonic fibroblasts (14). Our sequence analysis reveals that KLHL9 shares a high sequence homology of ∼90% with KLHL13, which may serve as the molecular basis for their shared substrate specificity toward IRS. Based on findings that Cul3 mediates IRS turnover in liver cells and that both KLHL9 and KLHL13 are expressed in livers (19) and AML12 cells, we further tested if knockdown of KLHL9 or KLHL13 recapitulate the insulin signaling enhancing effect of Cul3 knockdown in AML12 cells (Fig. 4 *I* and *J*). Protein levels of KLHL9 and KLHL13 could not be shown due to the lack of suitable antibodies obtained from multiple commercial sources. Indeed, knockdown of KLHL9 or KLHL13 resulted in increased IRS1 stability and enhanced insulin activation of AKT (Fig. 4 *I* and *J*), suggesting that KLHL9 and KLHL13 could serve as CRL3 substrate receptors for IRS1. In contrast, knockdown of another verified Cul3 substrate receptor KLHL21 (20), which shares only ∼30% sequence homology with KLHL9 and KLHL13, did not affect IRS1 protein stability or insulin activation of AKT (*SI Appendix*, Fig. S6). Taken together, these results provide additional evidence supporting the role of CRL1 and CRL3 in mediating IRS protein turnover, and substrate receptor redundancy exists in CRL-mediated IRS turnover in liver cells.

Hepatic Cul3 Deficiency, but Not Cul1 Deficiency, Stabilizes Hepatic IRS and Lowers Blood Glucose in Mice. To further determine if Cul1 and Cul3 also regulate hepatic IRS stability and blood glucose in vivo, we next knocked down Cul1 or Cul3 in mouse livers by using adeno-associated virus (AAV)-short hairpin RNA injection (Fig. 5 *A* and *B*). Knockdown of hepatic Cul1 resulted in only modest increase of IRS protein (Fig. 5*A*). In contrast, knockdown of hepatic Cul3 resulted in markedly increased hepatic IRS abundance (Fig. 5*B*). Consistently, hepatic Cul3 deficiency, but not hepatic Cul1 deficiency, significantly improved glucose tolerance in GTT (Fig. 5 *C–F*). These in vivo findings suggest that hepatic Cul3 may play a predominant role in mediating IRS turnover, and loss of hepatic Cul3 mimics the glucose lowering effect of MLN4924. In contrast, hepatic Cul1 deficiency only slightly increases hepatic IRS abundance, which does not result in glucose lowering in mice, possibly due to other compensatory degradation mechanisms including CRL3.

MLN4924 Intervention Attenuates Hyperglycemia Independent of Obesity in WD-Fed Mice. It is known that impaired IRS function is a major underlying cause of hepatic insulin resistance in fatty liver (6, 7). Consistently, we found strongly decreased hepatic IRS protein abundance in murine fatty livers induced by 12-wk WD feeding (Fig. 6*A*). While Cul1 neddylation appeared unaltered in fatty livers, neddylated Cul3 as well as Cul4A were increased while their unneddylated form was decreased in fatty livers (Fig. 6*A*). Fatty livers showed unaltered NAE1, the nedd8 E1 enzyme, but increased UBE2M (UBC12) (Fig. 6*A*), the major mammalian Nedd8 E2 enzyme that was recently reported to be induced under various cellular stress conditions (21), providing a possible explanation of hyperneddylation of some cullins in fatty livers (Fig. 6*A*). These findings led us to further

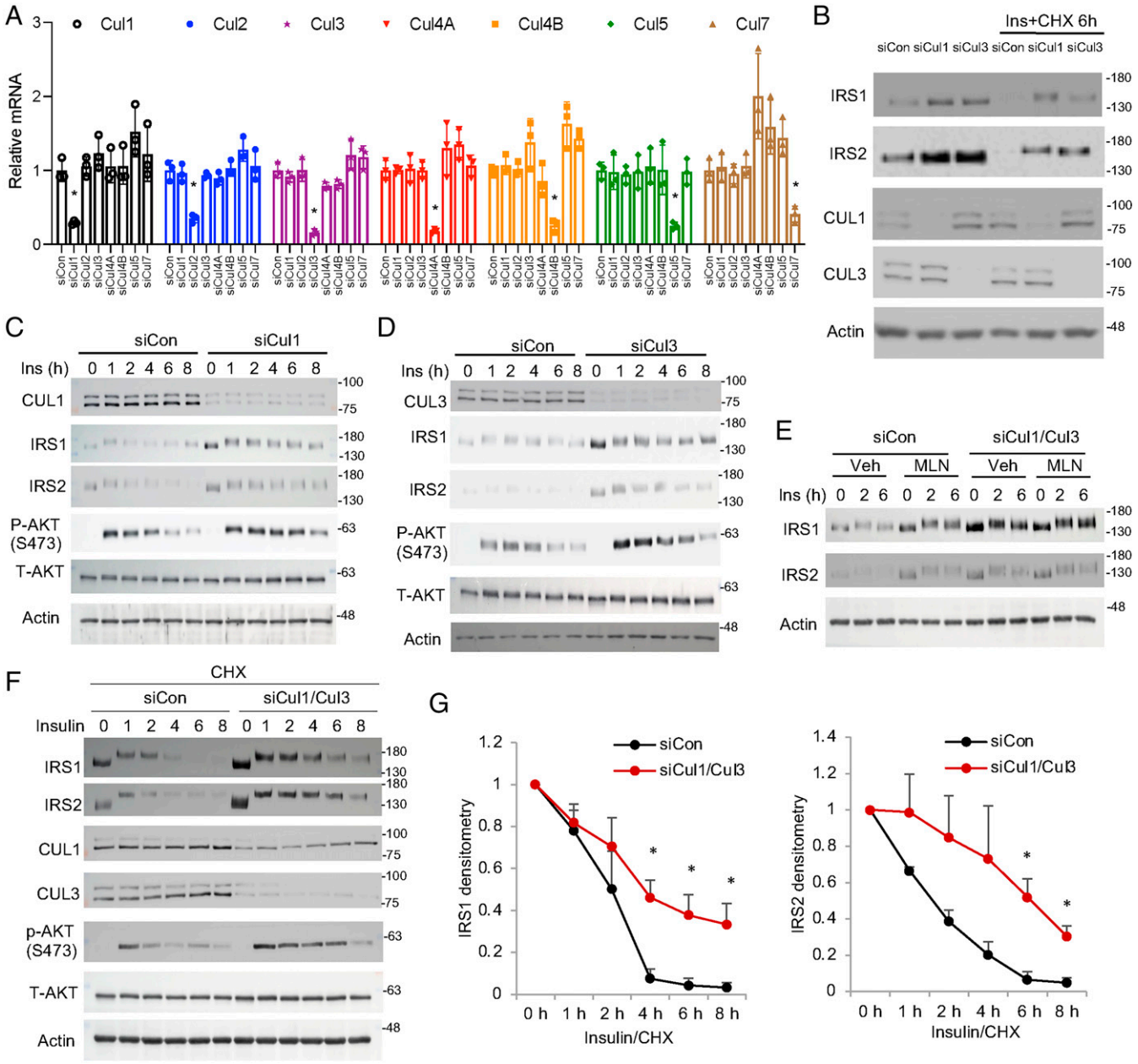

Fig. 3. Knockdown of Cul1 or Cul3 recapitulates the insulin sensitizing effect of MLN4924. (*A*) Knockdown of Cullin by siRNA in AML12 cells. Mean ± SD of three independent experiments. *$P < 0.05$ (unpaired Student's *t* test) versus siControl (siCon). (*B*) Western blot. Knockdown of Cul1 or Cul3 increases IRS1 protein abundance under basal culture condition or upon 6-h treatment of 100 nM insulin (ins) and 100 μg/mL CHX. (*C* and *D*) Western blot. Control and siCul1 or siCul3 knockdown AML12 cells were serum starved for 16 h followed by 100 nM insulin stimulation in time course. (*E*) Cul1 and Cul3 were simultaneously knocked down in AML12 cells by siRNA. Cells were serum starved for 16 h. Cells were then pretreated with vehicle (DMSO) or 500 nM MLN4924 for 1 h followed by 100 nM insulin treatment in time course. (*F*) Western blot. Cul1 and Cul3 were simultaneously knocked down in AML12 cells by siRNA. Cells were serum starved for 16 h followed by 100 nM insulin treatment in time course in the presence of 100 μg/mL CHX. (*G*) Relative densitometry of IRS protein as shown in *F*. Mean ± SEM of three independent experiments. *$P < 0.05$ versus siCon at the same time point. Unpaired Student's *t* test.

investigate the effect of pharmacological neddylation inhibition on glucose homeostasis under a pathologically relevant obesity setting. However, a recent study has reported that neddylation inhibition suppresses adipogenesis and MLN4924 administration via intraperitoneal (i.p.) injection significantly prevents obesity in high-fat diet–fed mice (22), which presents a major limitation in defining obesity-independent glucose lowering effect of chronic MLN4924 treatment. To circumvent this technical limitation, we validated a dosing protocol by employing SQ administration of MLN4924 (60 mg/kg, once every 2 d), which did not affect diet-induced obesity (Fig. 6*B*). This was possibly because SQ MLN4924 administration minimized direct visceral fat exposure to MLN4924 compared to i.p. injection. By using this dosing protocol, we found that MLN4924 treatment after 9 wk was still effective in reducing blood glucose in WD-fed mice without causing undesirable hypoglycemia in chow-fed mice (Fig. 6*C*). We found that 6-h fasting plasma insulin concentration showed significant variation in WD-fed mice and was not lowered in the MLN4924-treatment group (Fig. 6*D*). However, MLN4924 treatment significantly increased IRS protein and downstream AKT activation (Fig. 6 *E* and *F*). Consistently, MLN4924 treatment decreased hepatic gluconeogenic gene glucose 6-phosphatase

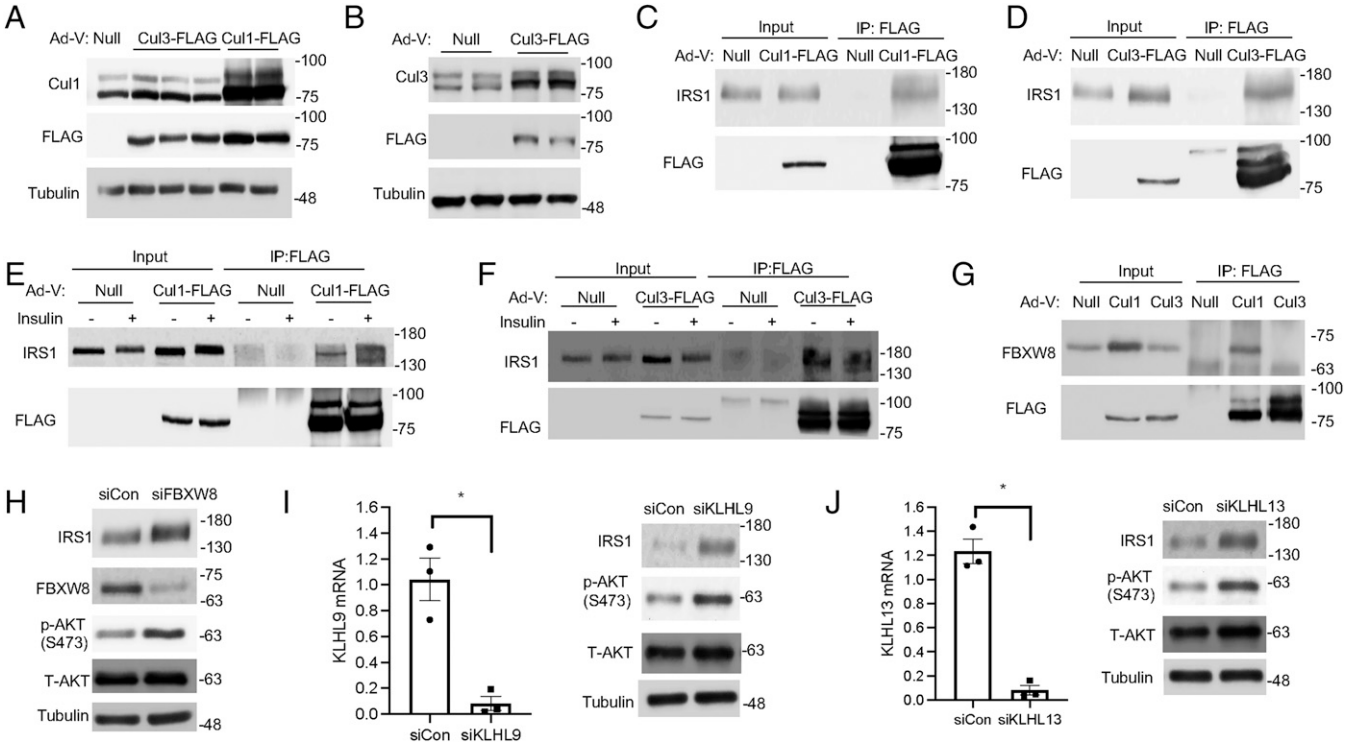

Fig. 4. CRL1 and CRL3 interact with IRS. (*A* and *B*) AML12 cells were infected with Ad-Null, Ad-Cul1-FLAG, or Ad-Cul3-FLAG at an MOI of 5 for 24 h, and Cul1-FLAG and Cul3-FLAG expression were confirmed by Western blot. Each lane represents cell lysate from an individual well of a 6-well plate. (*C* and *D*) AML12 cells infected with Ad-Null or Ad-Cul1-FLAG or Ad-Cul3-FLAG at MOI of 5. After 24 h, cells were then cultured in serum-free medium with MG132 (5 μM) for 8 h. IP was performed with anti-FLAG magnetic beads, and precipitated proteins were detected by immunoblotting. (*E* and *F*) AML12 cells were infected with Ad-Null, Ad-Cul1-FLAG, or Ad-Cul3-FLAG as indicated for 24 h. Cells were then cultured in serum-free medium with MG132 (5 μM) for 8 h. During the last 2 h, 100 nM insulin was added as indicated. IP was performed with anti-FLAG magnetic beads, and precipitated proteins were detected by immunoblotting. (*G*) AML12 cells were infected with Ad-Null, Ad-Cul1-FLAG, or Ad-Cul3-FLAG as indicated for 24 h. Cells were then cultured in serum-free medium with MG132 (5 μM) for 8 h. IP was performed with anti-FLAG magnetic beads, and precipitated proteins were detected by immunoblotting. (*H*) Western blotting. Control and siFBXW8 knockdown AML12 cells were serum starved for 16 h followed by 100 nM insulin stimulation for 6 h in the presence of 100 μg/mL CHX. (*I* and *J*) Control and siKLHL9 or KLHL13 knockdown AML12 cells were serum starved for 16 h followed by 100 nM insulin stimulation for 6 h in the presence of 100 μg/mL CHX. *Left* panel: mRNA expression. *Right* panel: Western blotting.

but not phosphoenolpyruvate carboxylase (Fig. 6*G*). Further characterization revealed that MLN4924 treatment significantly decreased hepatic fat content by ∼20% independent of adiposity or circulating fatty acids (Fig. 6*I* and *SI Appendix*, Fig. S7 *A–E*). Gene expression analysis showed that MLN4924 treatment decreased liver pyruvate kinase, a target gene of carbohydrate response element binding protein that is activated by high glucose to promote liver fat accumulation (23) (Fig. 6*H*). In contrast, MLN4924 treatment did not reduce key lipogenic genes fatty acid synthetase or acetyl-CoA carboxylase (*SI Appendix*, Fig. S7*F*). MLN4924 treatment did not cause alanine aminotransferase (ALT) elevation in chow-fed mice (Fig. 6*J*). Liver histology of chow-fed MLN4924-treated mice also appear to be comparable to controls (*SI Appendix*, Fig. S7*C*). Chronic WD feeding caused elevated ALT, which was reduced by MLN4924 treatment (Fig. 6*J*). These results suggest that chronic MLN4924 treatment did not cause detectable hepatotoxicity in chow-fed mice but significantly attenuated WD-induced liver injury. In summary, these results show that chronic MLN4924 treatment is effective in restoring hepatic insulin signaling and decreasing hyperglycemia independent of obesity in WD-fed mice.

Discussion

The major finding of this study is that neddylation inhibitors act as a glucose-lowering agent. This therapeutic effect can be attributed to enhanced hepatic insulin signaling and decreased glucose production but is independent of obesity reduction. This discovery builds on the well-established phenomenon that phosphorylation of IRS at multiple serine and threonine residues generate degron that is recognized by E3 ligases for ubiquitination and proteasome degradation (9, 12, 24–28). However, the broad cellular functions of these kinases present a major obstacle in directly targeting these kinases to improve insulin resistance (11). Recently, CRLs have been implicated in mediating IRS protein turnover in a few cell models (13, 14, 29). The unique feature of neddylation-mediated CRL activation has led to the development of pharmacological modulators of cellular CRL activity (5). In this study, we demonstrate that MLN4924 treatment significantly delays cellular feedback insulin desensitization by preventing the rapid CRL-mediated IRS protein turnover, leading to enhanced and prolonged hepatocellular response to insulin. This provides a mechanism of action of MLN4924-mediated insulin signaling activation, which is especially relevant to hepatic insulin–resistant conditions whereby the intrinsic signaling defect results from abnormally elevated proteasome degradation of IRS proteins. We demonstrate that short-term treatment was sufficient to cause significant reduction of blood glucose in WD-fed mice, suggesting that the glucose-lowering effect of MLN4924 is rapid and does not require significant reduction of obesity or hepatic fat content. Notably, MLN4924 mainly promotes cellular response to insulin stimulation but does not by itself cause undesirable persistent intracellular insulin signaling activation. Consistently, we

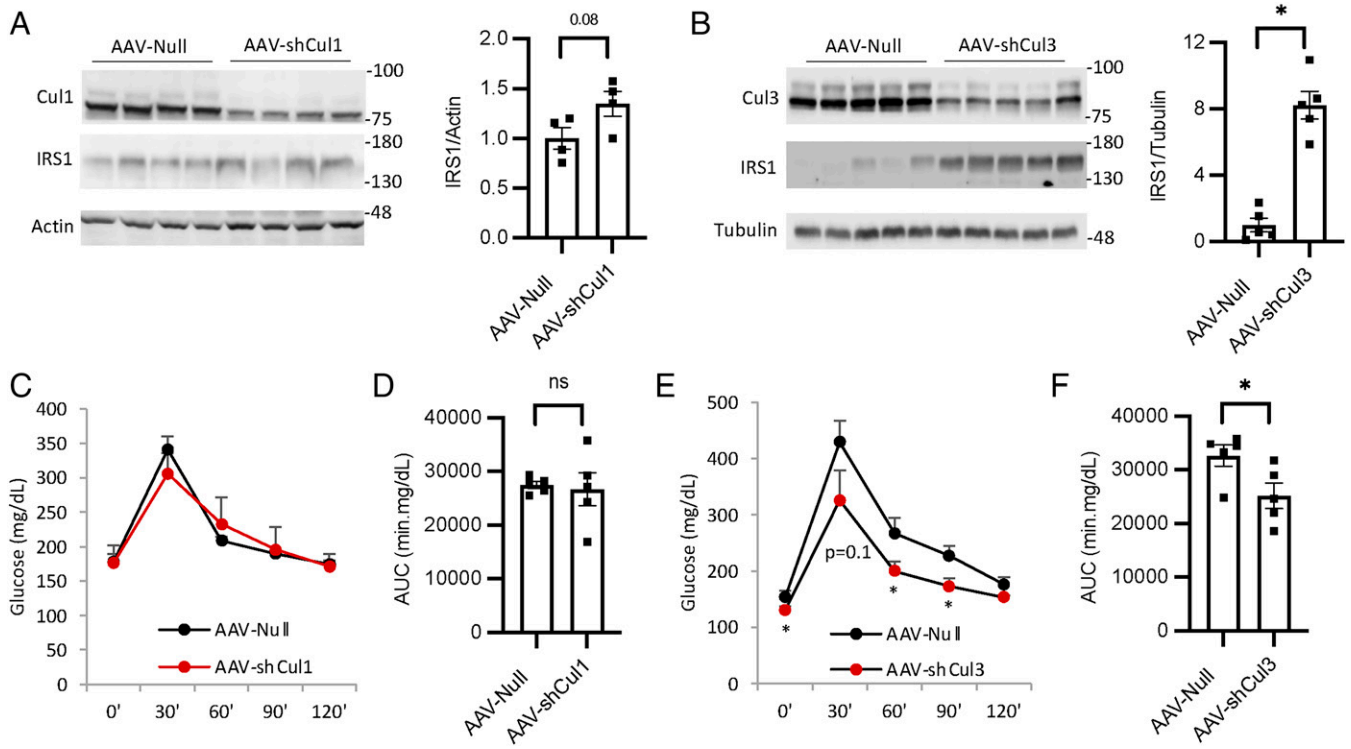

Fig. 5. Knockdown of liver Cul3, but not Cul1, increases IRS abundance and glucose tolerance in vivo. Chow-fed male C57BL/6J mice at 9 wk of age were intraperitoneally injected with AAV8-Null, AAV8-shCul1, or AAV8-shCul3 (2×10^{11}GC/mouse). GTT was performed at 4 to 5 wk postinjection. (*A* and *B*) Liver protein levels. Relative IRS1 protein densitometry is shown in the *Right* panel. (*C*–*F*) GTT and glucose area under the curve of GTT. All results are expressed as mean ± SEM ($n = 4$ to 5). *$P < 0.05$. Unpaired Student's *t* test was used to calculate the *P* value.

demonstrate that MLN4924 treatment does not cause hypoglycemia. MLN4924 treatment is associated with increased hepatic insulin signaling and decreased hepatic glucose production in mice. Although neddylation of noncullin proteins have been reported, cullins are considered the major neddylation targets under physiological conditions (2). In agreement with this, specific knockdown of Cul1 and Cul3 recapitulated the effect of MLN4924 in cultured cells, supporting that the effect of MLN4924 is largely mediated by cullins. This is further supported by the co-IP results demonstrating IRS1 association with Cul1 and Cul3. It was noted that insulin did not enhance IRS1 association with Cul1 or Cul3, despite that it is well-established that insulin-mediated IRS serine/threonine phosphorylation promotes its ubiquitylation and degradation (8, 9). However, this could potentially be due to the dynamic nature of the CRL and IRS interaction with rapid substrate dissociation from the receptors and the limitation of the co-IP experiment in capture such dynamic changes (17). Although knockdown of either Cul1 or Cul3 enhanced cellular insulin signaling in vitro, we found that only hepatic Cul3 deficiency significantly increased IRS abundance and lowered plasma glucose in vivo, mimicking the effect of MLN4924. In contrast, hepatic Cul1 knockdown only modestly increased hepatic IRS abundance, which was insufficient to lower glucose, suggesting that under in vivo conditions, CRL1 either plays a relative minor role in mediating hepatic IRS turnover or loss of Cul1 is compensated by other degradation mechanisms such as CRL3. Taken together, these findings suggest that pharmacological inhibition of cullin neddylation increases hepatic insulin signaling and lowers blood glucose, and thus represents a potential therapeutic strategy for nonalcoholic fatty liver disease (NAFLD)/type-2 diabetes.

We found that hepatic CRL neddylation is abnormally elevated in murine NAFLD livers, which correlated with significantly decreased hepatic IRS protein abundance. Increased hepatic cullin neddylation has also been reported in human fibrotic livers with different etiology (16), suggesting that hepatic hyperneddylation could be a pathologic stress response (21). Given that stress kinases–mediated S/T-phosphorylated IRS protein is recognized by CRL for ubiquitination, increased CRL activity may play a pathogenic role in promoting hepatic insulin resistance in NAFLD. Studies from liver-specific IR knockout mice and IRS knockout mice demonstrate that hepatic insulin resistance is not merely a consequence of obesity and NAFLD but critically contributes to systemic insulin resistance and dyslipidemia (7, 30, 31). As a result, hyperglycemia promotes hepatic steatosis, further contributing to hepatic insulin resistance and hyperglycemia in a vicious cycle. In this study, we showed that chronic MLN4924 treatment restored hepatic IRS abundance leading to increased hepatic AKT activation and simultaneously decreased hepatic fat accumulation in WD-fed mice. Along this line, it has recently been shown that MLN4924 treatment inhibited adipogenesis and prevented diet-induced obesity, leading to improved overall metabolic homeostasis in high-fat diet–fed mice (22). Compared to findings from this previous study, the ∼20% reduction of hepatic steatosis in our model was modest because of the lack of obesity alleviation, which is consistent with adipose-derived fatty acid being the major contributor to hepatic fat accumulation in obesity, while hepatic lipogenesis could be induced to contribute to a quarter of the hepatic fat content (32). However, analysis of hepatic gene expression did not identify a clear effect of MLN4924 on hepatic lipogenesis to account for reduced hepatic fat content, and how MLN4924 regulates hepatic lipid metabolism independent of obesity remains to be investigated. It should also be noted that chronic MLN4924 treatment in our model only reduced blood glucose but not plasma insulin levels in obese

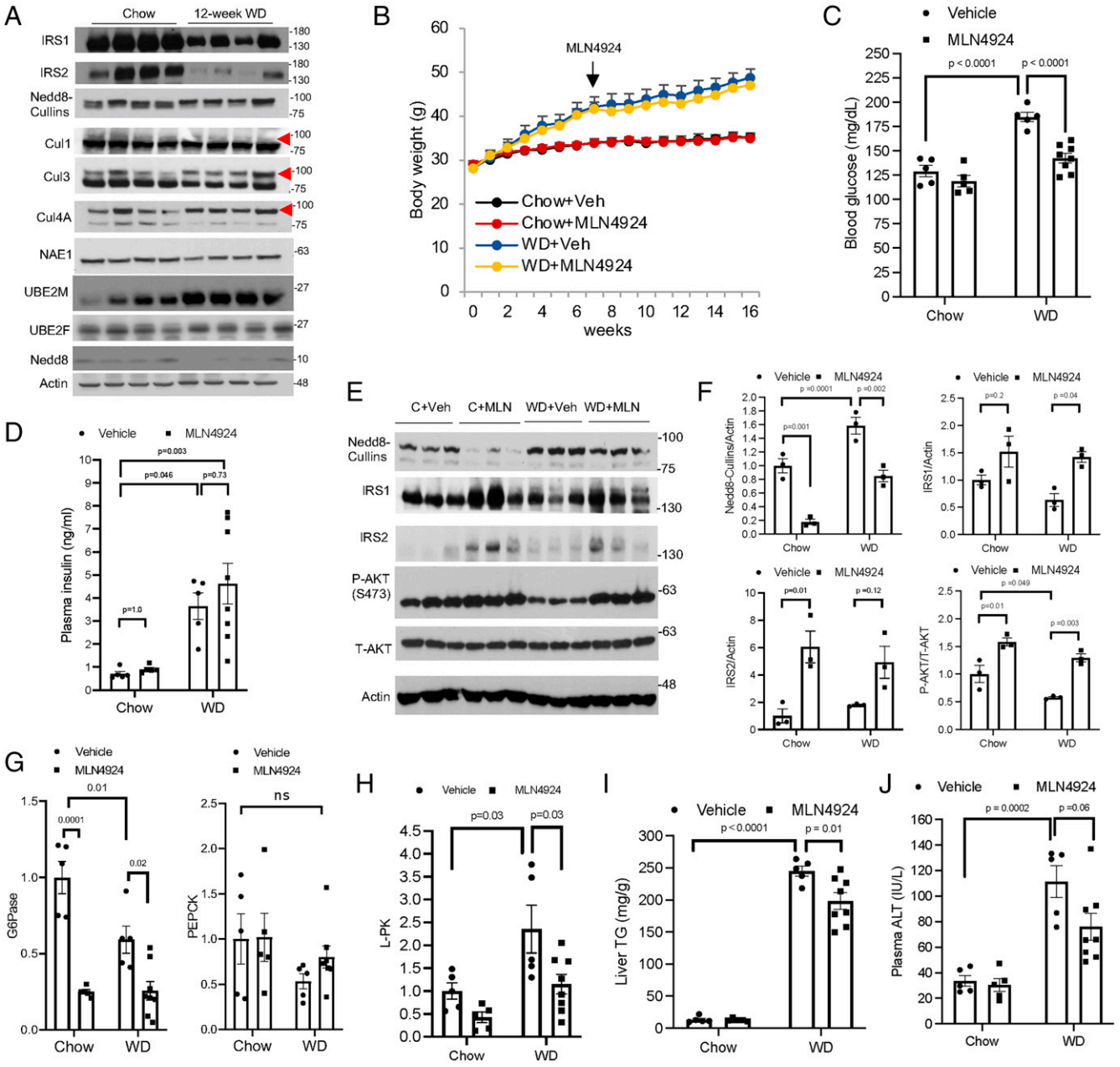

Fig. 6. Chronic MLN4924 treatment normalizes blood glucose independent of obesity in WD-fed mice. (*A*) Western blotting using liver lysate from male C57BL/6J mice fed chow or WD for 12 wk. The red arrow indicates neddylated cullin. (*B–J*) Male C57BL/6J mice were fed Chow or WD for 16 wk. MLN4924 treatment (60 mg/kg, SQ, every other day) was initiated after mice were fed WD for 7 wk as indicated. Control mice were injected with vehicle. After 16 wk of feeding, mice were fasted from 9 AM to 3 PM and euthanized. (*B*) Body weight. (*C*) Blood glucose was measured after 6-h fasting at time of euthanasia. (*D*) Plasma insulin. (*E* and *F*) Hepatic protein by Western blotting and densitometry analysis. (*G* and *H*) Relative liver mRNA expression. (*I*) Liver triglyceride content. (*J*) Plasma alanine aminotransferase (ALT). Results are expressed as mean ± SEM (n = 5 to 8). Two-way ANOVA and Tukey post hoc test were used to calculate the P value.

mice. In contrast, two previous studies showed that MLN4924 i.p. injection prevented diet-induced obesity, which reduced both plasma glucose and insulin (22, 33). These findings from us and others collectively suggest that MLN4924 treatment can acutely and robustly decrease plasma glucose independent of obesity, but reducing obesity by MLN4924 treatment achieves a higher degree of overall insulin sensitization.

It should be noted that cullins are implicated in embryonic and organ development, and global deletion of a cullin gene in mice, including Cul1, Cul3, and Cul7, causes embryonic and postnatal lethality (34–38), limiting further study of their function in these models. Given the versatile functions of CRLs, the absence of apparent adverse health impact upon MLN4924 treatment may be due to partial inhibition of hepatic neddylation and the lack of significant neddylation inhibition in other tissues such as the skeletal muscle, possibly due to poor MLN4924 distribution. In contrast, IRS turnover in hepatocytes appeared to be highly sensitive to neddylation inhibition, and only a partial reduction of cullin neddylation was sufficient to increase IRS protein and enhance hepatic insulin signaling in vitro and in vivo. These observations suggest that partial cullin neddylation pan-inhibition in a tissue-dependent manner

could lead to very different biological outcomes than complete genetic ablation of a single cullin protein, which may be an important reason that pharmacologically targeting cullin neddylation is a valid therapeutic approach for disease treatment.

The limitations of this study and future perspectives include that the substrate specificity of CRLs is largely determined by the substrate receptors in the CRL complex. In this study, we show that FBXW8 is a CRL1 substrate receptor that mediates IRS protein turnover in liver cells. However, further studies showed that hepatic Cul1 deficiency only caused moderate IRS increases and failed to lower glucose in vivo. In contrast, our in vivo findings suggest that hepatic Cul3 may play a predominant role in regulating IRS turnover to modulate insulin signaling. About 180 BTB-domain proteins could serve as a substrate receptor in a Cul3-containing CRL complex (1, 4). These receptors also exhibit tissue-specific expression patterns. Most of these receptors have not been functionally characterized to date, and their relative expression in hepatocytes is not fully clear. In addition to KLHL9 and KLHL13 that have been shown to recognize IRS protein, a systemic approach is still needed to identify additional substrate receptor(s) that mediate IRS protein turnover in hepatocytes and determine their physiological impact and functional redundancy on hepatic insulin signaling and glucose metabolism in vivo.

To date, CRLs have attracted attention mainly in cancer research owing to CRL regulation of oncogenes and tumor suppressors (4). Interestingly, recent studies suggest that neddylation inhibition attenuates hepatic steatosis, inflammation, and liver fibrosis in experimental models of fatty liver disease, cholestasis, and toxin-induced liver injury (16, 22). Furthermore, cullin hyperneddylation has also been linked to hepatocellular carcinoma progression and poor prognosis in humans (39–42). Therefore, targeting hepatic neddylation may potentially reduce NAFLD-associated liver cancer risk. These recent findings suggest that CRLs may be a potential therapeutic target for metabolic and inflammatory liver diseases, and future investigations are still needed to improve current knowledge on how CRLs modulate liver pathophysiology.

Materials and Methods

Reagents. MLN4924 and TAS4464 were purchased from MedChemExpress, Inc. Insulin (Novolin, national drug code 0169-1833-11) was purchased from Novo Nordisk Inc. CHX, wortmannin, Torin1, rapamycin, MG132, and antibodies against Nedd8 (No.2754, Lot. 2), Cul3 (No. 2759, Lot. 2), Cul4A (No.2699, Lot. 2), NAE1 (No. 14321, Lot. 1), p-IRβ (Y1150) (No. 3918, Lot.2), T-IRβ (No. 3025, Lot. 10), IRS1 (No. 2382, Lot. 10), IRS2 (No. 4502, Lot. 5), p-AKT(S473) (No. 4060, Lot. 24), p-AKT(T308) (No. 4056, Lot. 19), T-AKT (No. 4691, Lot.20), p-S6(S240/244) (No. 2215, Lot.14), T-S6 (No. 2217, Lot.5), p-4E-BP (T37/46) (No. 2855, Lot.20), T-4E-BP (No. 9452, Lot.10), Histone 3 (No. 9715S), were purchased from Cell Signaling Technology Inc. Antibodies against p-IRS1 (Y612) (No. 44-816G, Lot.SG255272), p-IRS1(S307), (No. PAI-1054, Lot.TG265968), Cul1 (No. 32-2400, Lot.UJ297298), and Cul2 (No. 51-1800, Lot.UA281866) were purchased from Invitrogen. Antibodies against Cul4B (No. 12916-I-AP) is purchased from Proteintech, Inc. FBXW8 (FBXO29, sc-514385, Lot.k0819), and UBE2F (sc-398668, Lot.G2916) antibodies were purchased from Santa Cruz Biotechnology, Inc. Antibodies against Cul7 (No. C1743, Lot.127M4759V) and 2-hydroxypropyl-b-cyclodextrin (No. 332607) were purchased from Sigma Aldrich. Antibodies against Actin (Ab3280) was purchased from Abcam. Insulin enzyme-linked immunosorbent assay kit (EZRMI-13K) was purchased from Millipore. ALT assay kit and triglyceride assay kit were purchased from Pointe Scientific. Fatty acid assay kit (K612) was purchased from BioVision, Inc. Lipofectamine RNAiMAX reagent was purchased from ThermoFisher Scientific.

Cell Culture and Transfection. AML12 cells were a generous gift from Dr. Yanqiao Zhang (Northeast Ohio Medical University, Rootstown, OH). Further cell authentication was not performed. AML12 cells were cultured in Dulbecco's modified Eagle's medium supplemented with a mixture of insulin-transferrin-selenium (No. 41400-045, ThermoFisher). For experiments, cells were cultured in serum-free medium overnight before various treatments were initiated. The siGENOME SMARTpool small interfering RNA (siRNA) and siControl were purchased from Dharmacon, Inc. The siRNA was transfected with Lipofectamine RNAiMAX reagent in a final concentration of 25 nM recommended by the manufacturer. Primary human hepatocytes and primary mouse hepatocytes were obtained from the Cell Isolation Core at the University of Kansas Medical Center. Treatments were initiated on the same day of isolation and completed within 24 h.

Co-IP. Adenovirus vectors Ad-Null, Ad-Cul1-FLAG, and Ad-Cul3-FLAG were purchased from Vector Biolabs Inc. AML12 cells were infected with Ad-Null, Ad-Cul1-FLAG, or Ad-Cul3-FLAG at an multiplicity of infection (MOI) of 5 as indicated for 24 h. Treatments were described in the figure legends. Cells were lysed in Co-IP buffer (20 mM Tris-Cl, pH = 7.5, 120 mM NaCl, 1 mM EGTA, 1 mM ETDA, 1% Nonidet P-40) supplemented with protease and phosphatase inhibitor mixture on ice for 1 h. Cell lysates were centrifuged at 10,000 × *g* for 10 min at 4 °C. Supernatant was transferred to a new tube, and 10% of the supernatant was saved as input. Anti-FLAG magnetic beads (Sigma-Aldrich) was added to the remaining supernatant. After overnight incubation with rotation at 4 °C, magnetic beads were washed in phosphate buffered saline (PBS)-T (1× PBS + 0.1% tween-20) five times. Immunoprecipitated proteins were eluted by incubating the magnetic beads in laemmli sample buffer at 80 °C for 5 min. Eluted protein lysates were used for sodium dodecyl sulphate–polyacrylamide gel electrophoresis (SDS-PAGE) and Western blotting.

Animal Experiments. Wild-type male C57BL/6J mice were purchased from the Jackson Lab. WD (TD. 88137, Envigo Inc.) contains 42% fat calories and 0.2% cholesterol. Mice were housed in microisolator cages with corn cob bedding under 7 AM–7 PM light cycle and 7 PM–7 AM dark cycle. MLN4924 was prepared in 10% 2-hydroxypropyl-b-cyclodextrin to a final concentration of 3 mg/mL. AAV vectors AAV8-Null, AAV8-shCul1, and AAV8-shCul3 were purchased from Vector Biolabs Inc. AAV was administered to mice via tail vein injection. All mice were fasted for 6 h from 9 AM to 3 PM before euthanasia. All animals received humane care according to the criteria outlined in the Guide for the Care and Use of Laboratory Animals (43). All animal protocols were approved by the Institutional Animal Care and Use Committee at the University of Kansas Medical Center and the University of Oklahoma Health Sciences Center.

Lipid Measurements. Lipids were extracted from liver tissues with a mixture of chloroform:methanol (2:1; volume:volume), dried under nitrogen, and resuspended in isopropanol containing 1% triton X-100. Liver triglyceride content was measured by a colorimetric assay kit following the manufacturer's instruction. Plasma fatty acid concentration was measured with a colorimetric assay kit following the manufacturer's instruction.

PTT, GTT, and ITT. On the day of testing, mice were fasted for 6 h from 9 AM to 3 PM. Mice were i.p. injected 2 mg/kg glucose for GTT, 2 mg/kg sodium pyruvate for PTT, and 0.5 U/kg insulin for ITT. Blood glucose was measured with a OneTouch Ultra glucose meter.

Tissue Lysate Preparation and Western Blotting. Tissue samples were homogenized in 1× radioimmunoprecipitation assay buffer (RIPA) buffer containing 1% sodium dodecyl sulfate (SDS) and protease inhibitors. Cultured cells were washed with ice-cold PBS and lysed in 1× RIPA buffer containing 1% SDS and protease inhibitors. After incubation on ice for 1 h, the samples were centrifugation, and supernatant was transferred to a new tube. The protein lysate was mixed with equal volume of 2× laemmli buffer and incubated at 95 °C for 5 min and used for SDS-PAGE and immunoblotting. ImageJ software (NIH) was used to determine band intensity.

RT-PCR. Total liver RNA was purified with TRIzol (Sigma-Aldrich). Total liver RNA was used in reverse transcription with Oligo dT primer and SuperScript III reverse transcriptase (Thermo Fisher Scientific). RT-PCR was performed on a Bio-Rad CFX384 RT- PCR system with iQ SYBR Green Supermix (Bio-Rad). The comparative CT method was used to calculate the relative messenger RNA (mRNA) expression. The relative mRNA expression was expressed as $2^{-\Delta\Delta Ct}$ with the control group arbitrarily set as "1."

Statistics. Unpaired Student's *t* test was used for two-group comparison. For multigroup comparison, one-way or two-way ANOVA and Tukey post hoc test were used. A $P < 0.05$ was considered statistically significant.

Data Availability. All study data are included in the article and/or *SI Appendix*.

ACKNOWLEDGMENTS. This study is supported in part by NIH Grant No. 1R01 DK117965-01A1 (T.L.) and 1R01 DK117418 (J.E.F.). We thank the Cell Isolation Core facility at the University of Kansas Medical Center Department of Pharmacology, Toxicology, and Therapeutics for providing primary human hepatocytes and primary mouse hepatocytes.

1. A. Sarikas, T. Hartmann, Z. Q. Pan, The cullin protein family. *Genome Biol.* **12**, 220 (2011).
2. R. I. Enchev, B. A. Schulman, M. Peter, Protein neddylation: Beyond cullin-RING ligases. *Nat. Rev. Mol. Cell Biol.* **16**, 30–44 (2015).
3. E. Bulatov, A. Ciulli, Targeting Cullin-RING E3 ubiquitin ligases for drug discovery: Structure, assembly and small-molecule modulation. *Biochem. J.* **467**, 365–386 (2015).
4. Y. Zhao, Y. Sun, Cullin-RING Ligases as attractive anti-cancer targets. *Curr. Pharm. Des.* **19**, 3215–3225 (2013).
5. T. A. Soucy *et al.*, An inhibitor of NEDD8-activating enzyme as a new approach to treat cancer. *Nature* **458**, 732–736 (2009).
6. D. Santoleri, P. M. Titchenell, Resolving the paradox of hepatic insulin resistance. *Cell. Mol. Gastroenterol. Hepatol.* **7**, 447–456 (2019).
7. X. Dong *et al.*, Irs1 and Irs2 signaling is essential for hepatic glucose homeostasis and systemic growth. *J. Clin. Invest.* **116**, 101–114 (2006).
8. K. D. Copps, M. F. White, Regulation of insulin sensitivity by serine/threonine phosphorylation of insulin receptor substrate proteins IRS1 and IRS2. *Diabetologia* **55**, 2565–2582 (2012).
9. T. Haruta *et al.*, A rapamycin-sensitive pathway down-regulates insulin signaling via phosphorylation and proteasomal degradation of insulin receptor substrate-1. *Mol. Endocrinol.* **14**, 783–794 (2000).
10. G. S. Hotamisligil, R. J. Davis, Cell signaling and stress responses. *Cold Spring Harb. Perspect. Biol.* **8**, a006072 (2016).
11. G. Solinas, B. Becattini, JNK at the crossroad of obesity, insulin resistance, and cell stress response. *Mol. Metab.* **6**, 174–184 (2016).
12. L. Rui, M. Yuan, D. Frantz, S. Shoelson, M. F. White, SOCS-1 and SOCS-3 block insulin signaling by ubiquitin-mediated degradation of IRS1 and IRS2. *J. Biol. Chem.* **277**, 42394–42398 (2002).
13. X. Xu *et al.*, The CUL7 E3 ubiquitin ligase targets insulin receptor substrate 1 for ubiquitin-dependent degradation. *Mol. Cell* **30**, 403–414 (2008).
14. S. Frendo-Cumbo *et al.*, Deficiency of the autophagy gene ATG16L1 induces insulin resistance through KLHL9/KLHL13/CUL3-mediated IRS1 degradation. *J. Biol. Chem.* **294**, 16172–16185 (2019).
15. C. Yoshimura *et al.*, TAS4464, a highly potent and selective inhibitor of NEDD8-activating enzyme, suppresses neddylation and shows antitumor activity in diverse cancer models. *Mol. Cancer Ther.* **18**, 1205–1216 (2019).
16. I. Zubiete-Franco *et al.*, Deregulated neddylation in liver fibrosis. *Hepatology* **65**, 694–709 (2017).
17. E. J. Bennett, J. Rush, S. P. Gygi, J. W. Harper, Dynamics of cullin-RING ubiquitin ligase network revealed by systematic quantitative proteomics. *Cell* **143**, 951–965 (2010).
18. I. Sumara *et al.*, A Cul3-based E3 ligase removes Aurora B from mitotic chromosomes, regulating mitotic progression and completion of cytokinesis in human cells. *Dev. Cell* **12**, 887–900 (2007).
19. S. Cirak *et al.*, Kelch-like homologue 9 mutation is associated with an early onset autosomal dominant distal myopathy. *Brain* **133**, 2123–2135 (2010).
20. S. Maerki *et al.*, The Cul3-KLHL21 E3 ubiquitin ligase targets aurora B to midzone microtubules in anaphase and is required for cytokinesis. *J. Cell Biol.* **187**, 791–800 (2009).
21. W. Zhou *et al.*, UBE2M is a stress-inducible dual E2 for neddylation and ubiquitylation that promotes targeted degradation of UBE2F. *Mol. Cell* **70**, 1008–1024.e6 (2018).
22. H. S. Park *et al.*, PPARγ neddylation essential for adipogenesis is a potential target for treating obesity. *Cell Death Differ.* **23**, 1296–1311 (2016).
23. H. Yamashita *et al.*, A glucose-responsive transcription factor that regulates carbohydrate metabolism in the liver. *Proc. Natl. Acad. Sci. U.S.A.* **98**, 9116–9121 (2001).
24. V. Aguirre, T. Uchida, L. Yenush, R. Davis, M. F. White, The c-Jun NH(2)-terminal kinase promotes insulin resistance during association with insulin receptor substrate-1 and phosphorylation of Ser(307). *J. Biol. Chem.* **275**, 9047–9054 (2000).
25. L. Rui *et al.*, Insulin/IGF-1 and TNF-alpha stimulate phosphorylation of IRS-1 at inhibitory Ser307 via distinct pathways. *J. Clin. Invest.* **107**, 181–189 (2001).
26. A. Takano *et al.*, Mammalian target of rapamycin pathway regulates insulin signaling via subcellular redistribution of insulin receptor substrate 1 and integrates nutritional signals and metabolic signals of insulin. *Mol. Cell. Biol.* **21**, 5050–5062 (2001).
27. C. J. Carlson, M. F. White, C. M. Rondinone, Mammalian target of rapamycin regulates IRS-1 serine 307 phosphorylation. *Biochem. Biophys. Res. Commun.* **316**, 533–539 (2004).
28. O. J. Shah, Z. Wang, T. Hunter, Inappropriate activation of the TSC/Rheb/mTOR/S6K cassette induces IRS1/2 depletion, insulin resistance, and cell survival deficiencies. *Curr. Biol.* **14**, 1650–1656 (2004).
29. J. Shi, L. Luo, J. Eash, C. Ibebunjo, D. J. Glass, The SCF-Fbxo40 complex induces IRS1 ubiquitination in skeletal muscle, limiting IGF1 signaling. *Dev. Cell* **21**, 835–847 (2011).
30. S. B. Biddinger *et al.*, Hepatic insulin resistance is sufficient to produce dyslipidemia and susceptibility to atherosclerosis. *Cell Metab.* **7**, 125–134 (2008).
31. M. D. Michael *et al.*, Loss of insulin signaling in hepatocytes leads to severe insulin resistance and progressive hepatic dysfunction. *Mol. Cell* **6**, 87–97 (2000).
32. J. C. Cohen, J. D. Horton, H. H. Hobbs, Human fatty liver disease: Old questions and new insights. *Science* **332**, 1519–1523 (2011).
33. H. Lin *et al.*, IP_6-assisted CSN-COP1 competition regulates a CRL4-ETV5 proteolytic checkpoint to safeguard glucose-induced insulin secretion. *Nat. Commun.* **12**, 2461 (2021).
34. U. Kossatz *et al.*, The cyclin E regulator cullin 3 prevents mouse hepatic progenitor cells from becoming tumor-initiating cells. *J. Clin. Invest.* **120**, 3820–3833 (2010).
35. J. B. Papizan, A. H. Vidal, S. Bezprozvannaya, R. Bassel-Duby, E. N. Olson, Cullin-3-RING ubiquitin ligase activity is required for striated muscle function in mice. *J. Biol. Chem.* **293**, 8802–8811 (2018).
36. Y. Wang *et al.*, Deletion of the Cul1 gene in mice causes arrest in early embryogenesis and accumulation of cyclin E. *Curr. Biol.* **9**, 1191–1194 (1999).
37. T. Arai *et al.*, Targeted disruption of p185/Cul7 gene results in abnormal vascular morphogenesis. *Proc. Natl. Acad. Sci. U.S.A.* **100**, 9855–9860 (2003).
38. J. D. Singer, M. Gurian-West, B. Clurman, J. M. Roberts, Cullin-3 targets cyclin E for ubiquitination and controls S phase in mammalian cells. *Genes Dev.* **13**, 2375–2387 (1999).
39. J. Yu *et al.*, Overactivated neddylation pathway in human hepatocellular carcinoma. *Cancer Med.* **7**, 3363–3372 (2018).
40. Z. Luo *et al.*, The Nedd8-activating enzyme inhibitor MLN4924 induces autophagy and apoptosis to suppress liver cancer cell growth. *Cancer Res.* **72**, 3360–3371 (2012).
41. Z. Yang *et al.*, Inhibition of neddylation modification by MLN4924 sensitizes hepatocellular carcinoma cells to sorafenib. *Oncol. Rep.* **41**, 3257–3269 (2019).
42. N. Embade *et al.*, Murine double minute 2 regulates Hu antigen R stability in human liver and colon cancer through NEDDylation. *Hepatology* **55**, 1237–1248 (2012).
43. National Research Council, *Guide for the Care and Use of Laboratory Animals* (National Academies Press, Washington, DC, ed. 8, 2011).